Carbohydrate Polymers 150 (2016) 308–318

Contents lists available at ScienceDirect

Carbohydrate Polymers

journal homepage: www.elsevier.com/locate/carbpol

Synthesis, characterization, and self-assembly with plasmid DNA of a quaternary ammonium derivative of pectic galactan and its fluorescent labeling for bioimaging applications

Ramesh Chintakunta[a,1], Nitsa Buaron[a,1], Nicole Kahn[a], Amana Moriah[d], Rinat Lifshiz[a], Riki Goldbart[a], Tamar Traitel[a], Betty Tyler[b], Henry Brem[b,c], Joseph Kost[a,*]

[a] Department of Chemical Engineering, Ben-Gurion University of the Negev, Israel
[b] Department of Neurosurgery, Johns Hopkins University School of Medicine, Baltimore, MD, USA
[c] Departments of Oncology, Ophthalmology, and Biomedical Engineering, Johns Hopkins University School of Medicine, Baltimore, MD, USA
[d] Department of Biomedical Engineering, Ben-Gurion University of the Negev, Israel

ARTICLE INFO

Article history:
Received 20 January 2016
Received in revised form 5 May 2016
Accepted 7 May 2016
Available online 10 May 2016

Keywords:
Pectic galactan
Quaternized pectic galactan
CHPTAC
5-DTAF
C6 rat glioma cells
Cell specific carrier

ABSTRACT

Quaternized derivatives of pectic galactan (QPG) were synthesized by a reaction of pectic galactan (PG) with 3-chloro-2-hydroxypropyl trimethyl ammonium chloride (CHPTAC) in the presence of aqueous sodium hydroxide solution under mild reaction conditions. The results showed that the concentration of CHPTAC and NaOH has great impact on the quaternization reaction. QPG was found to interact electrostatically with plasmid DNA in aqueous solution to form complexes in globular condensed morphology in a nanometer scale size ranging from 60 to 160 nm. Complexes formed with QPG fluorescently labeled with 5-DTAF (QPG-5-DTAF) were introduced to the C6 rat glioma cell line, and were found to be able to enter the cell and approach the nucleus within 24 h. The results suggest that this type of modified natural polysaccharide may have an advantage as a biocompatible and biodegradable gene delivery carrier and furthermore may serve as a cell specific carrier.

1. Introduction

In recent years, considerable attention has been focused on polysaccharides and their derivatives due to their application in the field of pharmaceutical chemistry as polymeric drug carriers, potential therapeutics, and some other useful applications (Hoffman, 2002; Gil, Li, Xiao, & Lowe, 2009; Samal et al., 2012; Edgar et al., 2001). Despite their useful applications, the most important issue of native non-ionic polysaccharides is insolubility in water as well as in most organic solvents. To circumvent this issue, it is essential to add an ionic moiety onto the native polysaccharide backbone. The addition of an ionic moiety does not change the fundamental properties of polysaccharides, but improves their physicochemical properties (Samal et al., 2012; Wang, & Xie, 2010). In particular, the addition of a cationic group onto polysaccharides enhances their water solubility and improves their potential to form electrostatic complexes with negatively charged molecules such as DNA, siRNA, and proteins. In addition, the cationic polysaccharides exhibit excellent biological properties including antitumor, antimicrobial, antioxidant, anti-inflammatory, and stimuli responsiveness (Sonia, & Sharma, 2011; Kim, H. W., Kim, B. R., & Rhee, 2010). Moreover, they are non-toxic, inexpensive, biocompatible, and easily biodegradable. Due to these properties they have been utilized in drug delivery (Cafaggi et al., 2007), siRNA delivery (Eliz et al., 2014), gene delivery (Yu, Huang, Ying, & Xiao, 2007; Yudovin-Farber & Domb, 2007), controlled release systems (Chaudhury and Das, 2011), and several industrial applications (Prado & Matulewicz, 2014; Heinze, Haack, & Rensing, 2004; Hashem, Hauser, & Smith, 2003; Pal, Mal, & Singh, 2008).

Quaternization is a very efficient process for the synthesis of cationic polysaccharides. Usually, the quaternized polysaccharides can be synthesized by the reaction of a polysaccharide with various cationic reagents possessing amino, imino, ammonium, phosphonium, and sulfonium groups (Solarek, 1986). Among these reagents, 3-chloro-2-hydroxypropyl trimethyl ammonium-chloride (CHPTAC) is a relatively inexpensive, low toxic, more stable, commercially available and environmentally friendly, therefore, this cationic reagent is widely used for the synthesis of

* Corresponding author.
E-mail address: kost@bgu.ac.il (J. Kost).
[1] These authors contributed equally.

http://dx.doi.org/10.1016/j.carbpol.2016.05.015
0144-8617/

quaternized ammonium polysaccharide. Quaternization with CHPTAC or 2,3-epoxypropyl trimethyl ammonium chloride (EPTAC) has been applied to various polysaccharides including starch (Eliz et al., 2014; Pal, Mal, & Singh, 2005; Wang et al., 2009), chitosan (Sajomsang, Tantayanon, Tangpasuthadol, William, & Daly, 2009; Cho, Grant, Piquette-Miller, & Allen, 2006), cellulose (Song, Sun, & Zhang, 2008; Niidei et al., 2010), xylans (Ebringerova, Hromadkova, Kacurakova, & Antal, 1994), konjac glucomannan (Yu et al., 2007), dextrin (Cho et al., 2013), pectin (Fan et al., 2012), and other biopolymers (Geresh, Dawadi, & Arad, 2000).

Pectic galactan (PG) is a complex copolysaccharide composed of galactose, arabinose, rhamnose, and galacturonic acid residues. In the PG, galactose is the main chain linked by a β-(1,4)-glycosidic linkage (Gunning, Bonraerts, & Morris, 2009). PG is abundant in plant cell walls, which is often attached to rhamnogalacturonan I (RG-I) as side chains. RG-I is a portion of the pectin backbone. A recent study shows that PG can play a critical role in cancer treatment (Gunning et al., 2009). We hypothesized that the quaternary ammonium derivative of PG could be synthesized by a reaction of PG with CHPTAC in the presence of aqueous sodium hydroxide solution. In this study, we report on the synthesis and characterization of a quaternary ammonium derivative of PG, its fluorescent labeling with 5-(4,6-dichlorotriazinyl) amino fluorescein(5-DTAF), and its possible application. Quaternized pectic galactan (QPG) might be useful in controlled release systems, targeted gene delivery, drug delivery, cosmetic, and pharmaceutical industries. Therefore, PG may become an important renewable resource for the synthesis of advanced cationic biomaterials.

2. Experimental

2.1. Materials

3-chloro-2-hydroxypropyl trimethyl ammonium chloride (CHPTAC, 348287), Sodium hydroxide (S-0399), dialysis cellulose membrane (D9652), phosphate buffered saline (PBS, P4417), deuteriumoxide-D_2O (151882), DMSO (dimethylsulfoxide, D2650), and KBr (221864) were purchased from Sigma-Aldrich Inc. Hydrochloric acid 32% (08460201), acetone (01030521), and ethanol (05250502) were purchased from Bio-Lab. PG (potato) (Lot Number PGAPT 80503c) was purchased from Megazyme International Ireland Ltd., Bray, Ireland. The monosaccharide composition was provided by the company (galactose: 82%, arabinose: 6%, rhamnose: 3%, and galacturonic acid: 9%).We have illustrated simplified chemical structures (reaction schemes and figures) of a complex copolysaccharide (PG). 5-(4,6-dichlorotriazinyl) aminofluorescein (5-DTAF-single isomer) was purchased from Molecular Probes Life Technologies.Ampicillin sodium salt (A9518), Tris base (T6791), Ethylenediaminetetraacetic acid (EDTA) pH = 8 (E1644), and tryptose phosphate broth (T9157) were purchased from Sigma. Plasmid purification Jetstar Maxi Kit (220010) was purchased from Genomed, Germany. Sea Kem LE Agarose (50004) was purchased from Lonza, USA. Blue/orange 6 × loading dye (G190A) and 1 kb DNA ladder (G571A) were purchased from Promega, USA. Ethidium bromide (EtBr) (E73298) was purchased from Tamar, Israel. Glacial acetic acid (8762) was from Gadot Biochemical Industries Ltd., Israel. TAE (Tris-acetate-EDTA) electrophoresis buffer was prepared routinely in our lab as 50 × stock solution, by mixing 242 g Tris base, 57.1 mL glacial acetic acid, and 100 mL of 0.5 M EDTA pH = 8. Cell culture Dulbecco's Modified Eagle's Medium (DMEM) (01-055-1A), fetal bovine serum (04-121-1A), Pen-strep (03-031-1B), L-glutamine (03-020-1B), and trypsin (03-052-1B) were purchased from Biological Industries, Israel. Wheat germ agglutinin, Alexa Fluor 555 conjugate (W32464), Hank's balanced salt solution (HBSS) (14175-079), and Prolong gold antifade reagent with DAPI (P36935) were purchased from Invitrogen, Rhenium Ltd, Israel.

2.2. Measurements

NMR spectra (^1H and ^{13}C) were recorded on a 500 MHz Brucker spectrometer. Chemical shifts are reported in parts per million (ppm) and referenced to the NMR solvent signals (D_2O). The FT-IR spectra were obtained in a Thermo-Nicolet FT-IR Spectrophotometer (Model-Nicolet iS10 FT-IR). For FT-IR measurement, the potassium bromide (KBr) pellet method was used. The spectra were obtained in the region from 4000 to 500 cm^{-1} with a resolution of 4 cm^{-1}. The nitrogen content (%N weight) was measured by elemental analysis, performed with a Carlo Erba 1108 elemental analyzer. Fluorescence spectra were recorded on a TECAN (Micro plate reader) infinite M200 spectrophotometer. The sample was dissolved in 0.1 M NaOH solution. TGA was performed in a simultaneous Mettler-Toledo Thermal Gravimetric Analyzer with a scanning rate of 10 °C min^{-1} under N_2 (g) atmosphere with flow of 20 mL min^{-1} in a temperature range of 25–600 °C. The degree of substitution (DS) of the QPG derivatives was calculated from the nitrogen content according to Eq. (1).

$$DS = \frac{162 \times N\%}{14 \times 100 - 151.5 \times N\%} \quad (1)$$

where 162 is the molecular weight of anhydroglucose units (AGU) of PG, N is the amount of nitrogen estimated from elemental analysis, 151.5 is the molecular weight of 2,3-epoxypropyl trimethyl ammonium chloride (EPTAC), and 14 is the molecular weight of nitrogen.

2.3. General procedure for the synthesis of the QPG

Briefly, sodium hydroxide (0.950 g, 0.0237 mol) was dissolved in 5.0 mL of double distilled water (DDW), and then PG (0.250 g, 0.0015 mol) was added portion-wise into the above solution. The reaction mixture was stirred continuously for 30 min at room temperature, then the cationic reagent, CHPTAC (4.60 g, 0.0244 mol) mixed in 10 mL of double distilled water (DDW) was added dropwise into the above reaction mixture and stirring was continued for 24 h at room temperature. The product was precipitated in an acidified mixture of ethanol and acetone (0.8 mL of hydrochloric acid + 20 mL of ethanol + 59.2 mL of acetone). The precipitate was washed with 80% ethanol (10 mL DDW + 40 mL ethanol), dissolved in a small volume (1–2 mL) of DDW, and then purified by dialysis through a 14 kDa cut-off dialysis bag that was placed in a vessel containing 5.0 L of DDW. The water was replaced four times with fresh DDW during 48 h of dialysis. The dialyzed product was then dried by lyophilization for 72 h to obtain the purified QPG. Experiments were conducted under different moles of NaOH and CHPTAC to obtain seven QPG derivatives, which coded as QPGs.

2.4. Procedure for the fluorescent labeling of QPG

In a typical experiment, 100 mg of QPG was dissolved in 3.0 mL of DDW, and then the pH was adjusted with 1.0 M NaOH to 11–12 and the mixture was stirred for 30 min at room temperature. After 30 min, a sample of 7.5 mg of 5-DTAF in DMSO (0.3 mL) was added to the above QPG solution and stirred for an additional 24 h at room temperature in the dark. After 24 h, the reaction mixture was neutralized with 0.2 M HCl and poured into a dialysis bag. The QPG-5-DTAF was separated from free 5-DTAF by extensive dialysis against phosphate-buffered saline (PBS) solution (pH 7.5) for 72 h and then against DDW for 48 h. The dialyzed product was then freeze dried and lyophilized for 72 h to obtain the purified QPG-5-DTAF.

2.5. Plasmid DNA purification

Plasmid pSuperneo (5429 bp) encoding for green fluorescence protein (pGFP) was routinely isolated from ampicillin-resistant DHM-α *Escherichia coli*. The DNA was amplified in tryptosephosphate broth containing 0.2 mg/mL ampicillin for 24 h before isolation, using bacteria that were frozen (−78 °C) in 40% glycerol. Isolation procedure was performed using a plasmid purification MAXI kit. A Nanodrop spectrophotometer (NanoDrop® ND-1000) was used to quantify the concentration of the obtained DNA.

2.6. Complex formation and gel electrophoresis assay

Complex formation was evaluated as a function of N/P ratio, calculated from the molar ratio between the cationic amine groups on the QPG (N) and the anionic phosphate groups on the pGFP (P). According to the desired ratio, an appropriate quantity of QPG (in DDW) at concentration of 0.1 μg/μL was introduced into a tube containing pGFP solution. The tube was incubated for 1 h until complexation was established, and complex formation was determined by gel electrophoresis (Wide Mini-Sub cell GT, BioRad). The complexes were diluted by DDW to a final volume of 12–18 μL. Loading buffer was added at sufficient volume to dilute the samples 6 times. The Complexes were loaded on 0.8% agarose gel (containing 1.6 μL/100 mL TAE buffer) containing ethidium bromide. In addition, DNA ladder and free pGFP were loaded as controls. The gel was exposed to an electric field for 45 min, and then visualized and photographed under UV illumination (Visible and Ultraviolet Transilluminator, DNR Bio-Imaging Systems).

2.7. Nanoparticle tracking analysis (NTA)

Complexes at desired N/P ratio were prepared at a final concentration of 3 μg/mL and were measured by the NanoSight's NS300 instrument equipped with a 405 nm laser module and 450 nm long pass filter. The samples were injected into the sample chamber with sterile syringes until the liquid reached the tip of the nozzle. All measurements were performed at room temperature. The software used for capturing and analyzing the data was the NTA 2.3 version (NanoSight Ltd.). All samples were analyzed under 20 × objective; 60-s video clips were taken.

2.8. TEM at cryogenic temperature (cryo-TEM)

Complexes at desired N/P ratio were prepared and 3 μL of each sample was dripped onto a copper grid coated with a perforated lacy carbon 300 mesh (Ted Pella Inc.) and blotted with filter paper to form a thin liquid film of solution. The blotted samples were immediately plunged into liquid ethane at its freezing point (−183 °C). The procedure was performed automatically in the Plunger (Lieca EM GP). The vitrified specimens were transferred into liquid nitrogen for storage. The samples were studied using a FEI Tecnai 12 G2 TEM, at 120 kV with a Gatancryo-holder maintained at −180 °C, and images were recorded on a slow scan cooled charge-coupled device CCD camera (GatanInc., USA). Images were recorded with the Digital Micrograph software package, at low dose conditions to minimize electron beam radiation damage.

2.9. Cell culture

C6 rat glioma cell line was used as the cancer cell model. Cells were grown in DMEM containing 10% fetal bovine serum, 1% Penicillin-Streptomycin, and 1% L-glutamine on uncoated flasks at 37 °C under 5% CO_2 atmosphere. Cells were passaged every 72–96 h. Cells were frozen in fetal bovine serum with 7.5% DMSO.

2.10. Incubation of cells with complexes

Cells were seeded at a density of 100,000 cells/mL and grown to ~70% confluence in a 24-well plate with a 13 mm glass coverslip; 0.5 μg DNA was used per well. Labeled complexes were prepared, and after 1 h incubation were diluted for a total volume of 250 μL with DDW. Complexes were dripped into wells containing 250 μL clean DMEM and after 4 h of incubation the serum-free medium was replaced with fresh medium containing serum (10% serum, 1% L-glutamine, 1% Pen-Strep in DMEM), and incubated for an additional 24 h. Cells were labeled and fixed according to protocols listed below. Fluorescence images were acquired on the OLYMPUS FluoView-1000 laser-scanning confocal microscope using a UPLSAPO 60x O (NA: 1.35) objective.

2.11. Fluorescent labeling of membrane

Cell membrane was labeled using wheat germ agglutinin Alexa Fluor 555 conjugate according to the manufacturer's protocol for labeling live eukaryotic cells.

2.12. Fluorescent labeling of nucleus

The nucleus was labeled using Prolong gold antifade reagent with DAPI; one drop of reagent was added on a glass slide. Coverslip sample was placed onto the reagent on the glass slide. Sample was placed for 24 h at room temperature in the dark.

2.13. Cell fixation

Cells were fixated by adding 300 μL Para formaldehyde 4% per well, followed by incubation for 15 min in the dark at 37 °C. Then, the solution was removed and the wells were rinsed three times with HBSS.

3. Results and discussion

3.1. Synthesis of the QPG

The reaction scheme and mechanism for the synthesis of QPG are shown in Scheme 1. As can be seen, the PG was treated with cationic reagent (CHPTAC) in the presence of aqueous sodium hydroxide solution at room temperature for 24 h. Under the present reaction condition, the reaction proceeded smoothly and provided QPG. The reaction mechanism proceeds in three steps. In step-I, the PG was activated in the presence of aqueous NaOH solution. In step-II, the CHPTAC was converted into its corresponding epoxide (EPTAC) via NaCl elimination in the presence of aqueous NaOH solution. In step-III, the activated PG (A-PG) attacks at the least substituted carbon of the epoxide ring under basic condition to give QPG.

In order to determine the exact quantity of CHPTAC as well as NaOH needed for the reaction, we optimized the reaction condition by varying the quantity of CHPTAC as well as NaOH with respect to a given weight of PG (0.0015 mol). Despite the increased molar equivalent of CHPTAC, the concentration of CHPTAC stays the same for all the reactions. The obtained results are summarized in Table 1. Our optimum conditions involved a reaction using 0.0122 mol of CHPTAC and 0.0119 mol of NaOH, with 0.0015 mol of PG in water at room temperature for 24 h (Table 1, entry 2). It is noteworthy that the concentration of NaOH influences the degree of substitution. With the increase in NaOH concentration, the DS value decreased (Table 1, entries 5–6). At high NaOH concentration, a side reaction of CHPTAC with NaOH could take place, forming the vicinal diol as a by-product by the hydrolysis of the epoxide (Kavaliauskaite, Klimaviciute, & Zemaitaitis, 2008). Moreover, it was revealed that

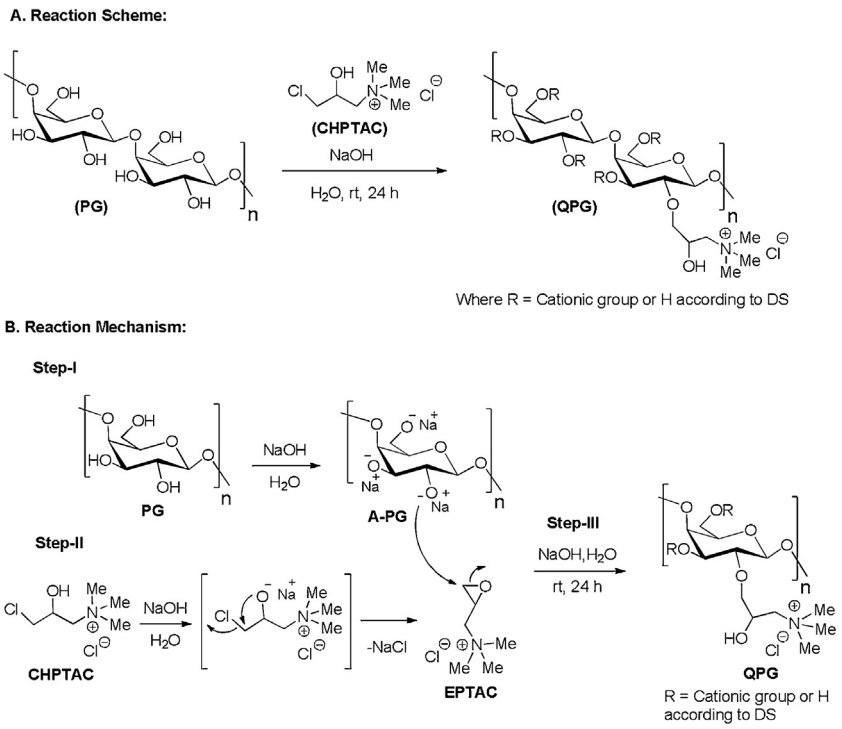

Scheme 1. Reaction scheme and mechanism for the quaternization of PG with CHPTAC.

Table 1
Optimization results of quaternary ammonium derivatives of PG.

Entry	PG (mol)[a]	NaOH/H_2O (mol/mL)[b]	Sample ID	Degree of Substitution (DS)[c]
1	0.0015	0.0059/1.4	QPG-1	0.51
2	0.0015	0.0119/2.5	QPG-2	0.53
3	0.0015	0.0179/3.7	QPG-3	0.51
4	0.0015	0.0238/5.0	QPG-4	0.50
5	0.0015	0.0119/2.5	QPG-5	0.07
6	0.0015	0.0146/2.5	QPG-6	0.41
7	0.0015	0.0171/2.5	QPG-7	0.36

[a] Calculated on the basis of anhydroglucose units (AGU) of PG. 1 mol AGU = 162 g.
[b] The molar equivalents of CHPTAC to NaOH (for entries 1–4: 1.03, for entries 5, 6, 7: 2.06, 0.85 and 0.72 equivalents, respectively).
[c] DS was calculated based on the nitrogen percentage.

excess use of CHPTAC did not increase the degree of substitution of QPG under the present reaction conditions (Table 1, entries 3–4). At higher molar ratio of CHPTAC with lower molar ratio of NaOH, the DS value rapidly decreased (Table 1, entry 5). This may be due to the use of lower concentration of NaOH, the complete conversion of CHPTAC to epoxide could not take place, therefore, the DS value decreased (Fan et al., 2012). According to our optimization results, the maximum DS of QPG 0.53 and minimum of 0.36 were observed.

3.2. Characterization of the QPG by ^{13}C NMR, FT-IR, TGA and elemental analysis

The ^{13}C NMR spectra of CHPTAC, PG, and QPG are shown in Fig. 1. The peaks of CHPTAC, anhydroglucose units of PG, and QPG were assigned based on previous reports (Song et al., 2008; Yu et al., 2007; Gong, Wang, & Tu, 2006; Synytsya et al., 2004). From the spectrum of the CHPTAC (Fig. 1A), the most significant peak for C-4 at 54.1 ppm is ascribed to the three methyl carbons of the quaternary ammonium group. The peaks at 68.2, 65.5, and 46.9 ppm are assigned to the C-1, C-2, and C-3 carbons of the reagent, respectively. In the spectrum of PG (Fig. 1B), the peaks related to C-1, C-5, C-3, C-2, C-4, and C-6 appear at 104.3, 77.6, 74.5, 73.3, 71.8, and 60.7 ppm, respectively(Gunning et al., 2009). In QPG spectrum (Fig. 1C), the signals at 104.4 and 103.6 ppm are attributed to C-1. The chemical shifts at 77.6, 76.6, 74.4, 71.8, and 60.7 ppm are attributed to C-5, C-2, C-3, C-4, and C-6, respectively. The peaks at 73.2, 68.2, and 65.0 ppm are assigned to C-7, C-9, and C-8, respectively. A sharp and intense signal at 54.1 ppm is assigned to the methyl carbons of the quaternary ammonium group (C-10), which exist in QPG and are absent in native PG. The existence of methyl carbons of the quaternary ammonium group in QPG proved the successful synthesis of QPG. The major component of pectic galactan is galactose and quaternization is therefore expected to take place primarily on the hydroxyl groups of galactose. Based on our ^{13}C NMR data and previous reports (Wang et al., 2009), the quaternization can take place on the C2 hydroxyls of galactose.

The FT-IR spectra of PG and QPG are shown in Fig. 2. From the FT-IR spectrum of the PG (Fig. 2A), the absorption bands at 1229, 1055, and 890 cm^{-1} relate to the C—O bond stretching vibration of the anhydroglucose units (AGU). The absorption bands at 2929 and 1626 cm^{-1} are characteristic absorption bands of the C—H stretching vibration and first overtone of O—H bending vibration, respectively. The broad and strong absorption band at 3401 cm^{-1} is the characteristic absorption band of the hydroxyl group stretching vibration. In the case of QPG (Fig. 2B), the quaternary ammonium group stretching vibration band appeared at 1479 cm^{-1}, which confirms the incorporation of a cationic group onto the PG.

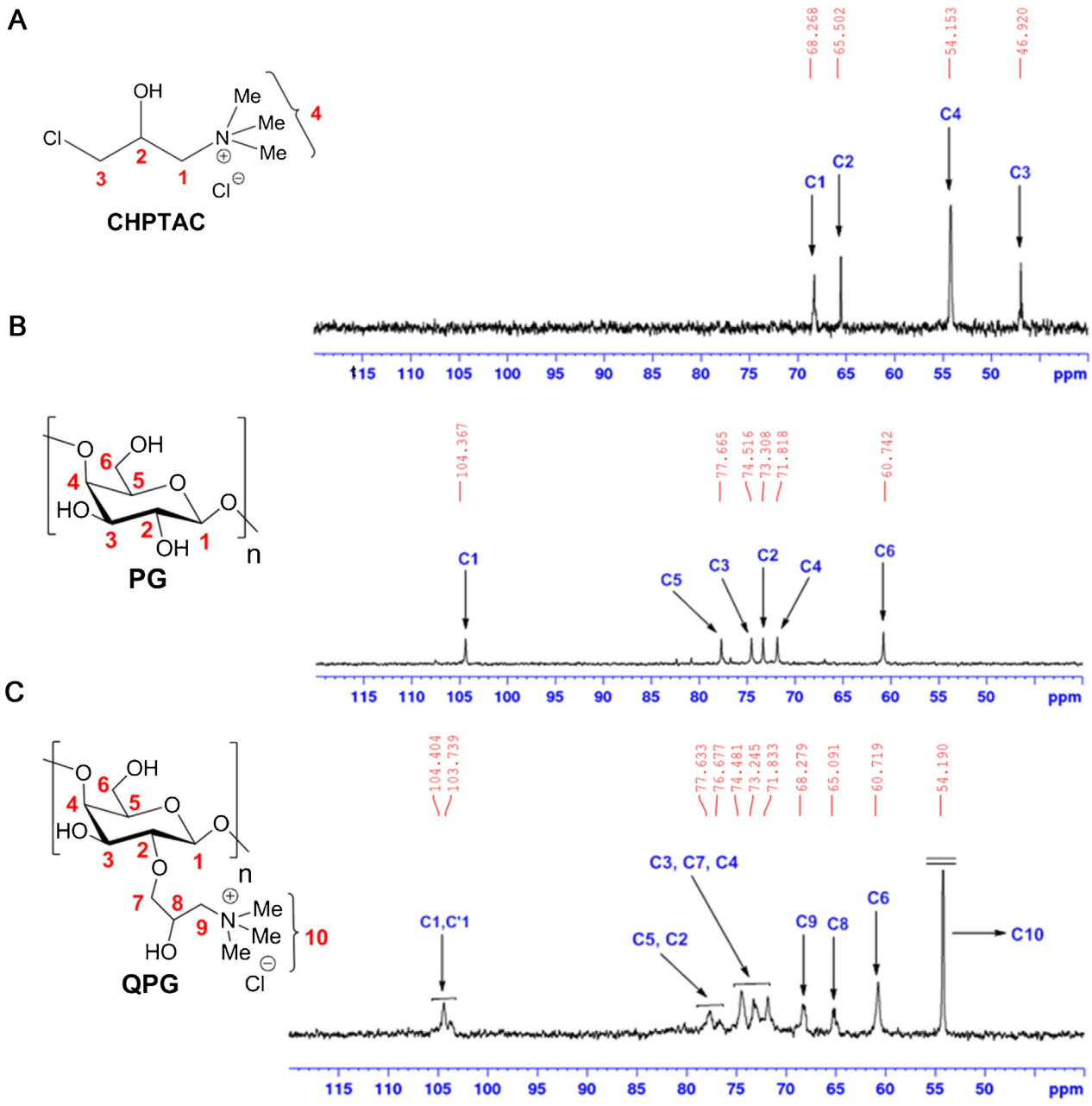

Fig. 1. ^{13}C NMR spectra of CHPTAC (A), PG (B), and QPG (C).

The Thermo gravimetric Analysis (TGA) spectra of PG and QPG obtained at a scan rate of 10 °C min^{-1} under nitrogen atmosphere are shown in Fig. 3. In the case of PG (Fig. 3A), the weight loss takes place in two stages. In stage one, 11.1% of the weight loss occurs between 31 and 187 °C, which is due to the presence of a small amount of moisture and other volatile compounds, with maximum weight loss at 49.2 °C. In stage two, 71.7% of the weight loss occurs between 187and 400 °C, which is due to the thermal degradation of polymer rings and disintegration of polymer chains, with maximum weight loss at 305.8 °C. Beyond 400 °C, degradation proceeds at a very slow rate up to 600 °C, leaving about 11.5% of the residual weight. In the case of QPG (Fig. 3B), the weight loss of the polysaccharide occurs in three distinct zones. As per PG, the initial stage of QPG weight loss (7.4%) is due to a small amount of moisture in the product at temperatures between 30 and 120 °C, with maximum weight loss at 45.2 °C. In stage two, 36.8% of the weight loss occurs between 150 and 302 °C, which is due to thermal degradation of the quaternary ammonium group side chain of the polymer, with maximum weight loss at 283.2 °C. In stage three, 41.0% of the weight loss (302–416 °C) is due to the decomposition of the cyclic rings of the polymer. The maximum weight loss at this stage occurs at 330.1 °C. Beyond this temperature (416 °C), the rate of weight loss is very slow and gradual upto 600 °C, leaving about 10.3% of the residual weight. The TGA results indicated that QPG is thermally more stable compared to PG (Pal et al., 2008). May be due to the intra molecular hydrogen bonding between hydroxyl groups of grafted side chains with oxygen of polymer ring may increase the thermal stability of QPG.

The elemental analysis results are presented in Table 2. The native PG does not contain any significant amount of nitrogen or chloride, whereas considerable quantities of nitrogen and chloride are present in the derivatives of QPG. The presence of nitrogen

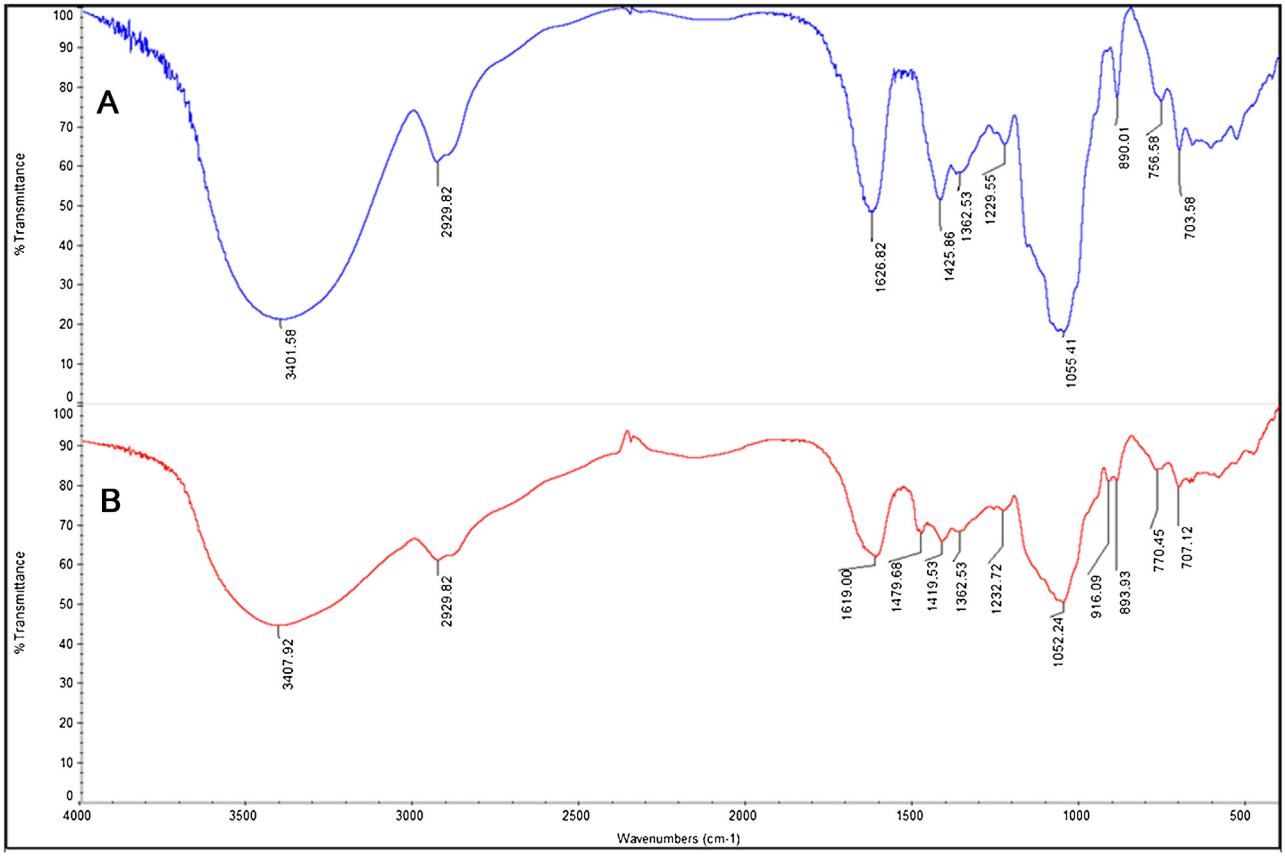

Fig. 2. FT-IR spectra of PG (A) and QPG (B).

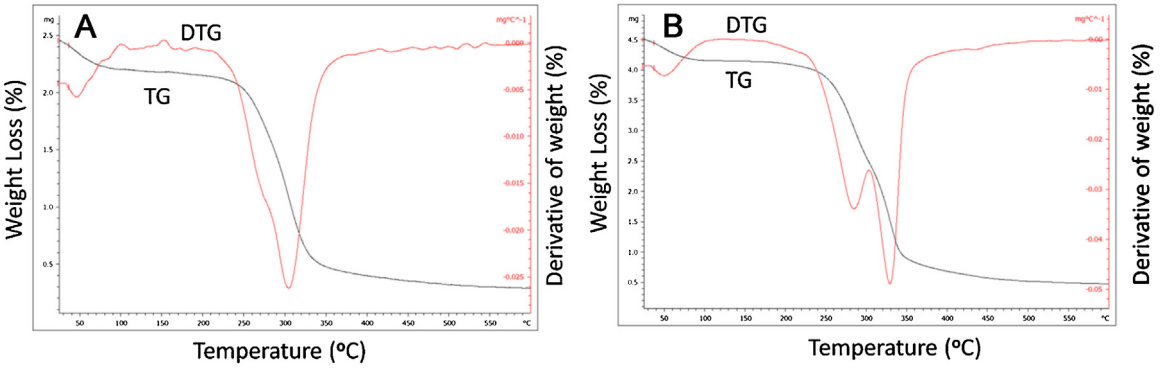

Fig. 3. TG and DTG curves for PG (A) and QPG (B).

Table 2
Elemental analysis results of the PG and QPG derivatives.

Sample ID	Carbon (%)	Hydrogen (%)	Nitrogen (%)	Chloride (%)
PG	37.98	6.44	0.00	0.00
QPG-1	37.91	7.66	2.99	5.63
QPG-2	39.97	7.50	3.08	6.21
QPG-3	40.29	7.64	2.99	4.96
QPG-4	40.91	7.81	2.94	5.81
QPG-5	38.21	6.77	0.61	0.59
QPG-6	40.20	7.73	2.57	2.11
QPG-7	40.18	7.52	2.34	2.00

and chloride is an additional proof of incorporation of quaternary ammonium group onto the PG. We proved the incorporation of the quaternary ammonium group onto the PG based on the FT-IR, ^{13}C NMR, TGA, and elemental analysis results.

3.3. Fluorescent labeling of QPG

Recently, random covalent attachment of fluorophores to the polymer has gained significant interest due to their useful application in visualizing the polymer location in in vitro or in vivo experiments (Abitbol, Palermo, Moran-Mirabal, & Cranston, 2013; Dong & Roman, 2007; Gunning et al., 2009). In this regard, we adapted a previously reported procedure with a slight modification for the covalent attachment of 5-DTAF to the QPG (Gunning et al., 2009). Our approach for the fluorescent labeling of QPG with 5-DTAF is presented in Scheme 2. QPG was treated with 5-DTAF at basic pH (11–12) in the dark at room temperature for 24 h. Under the present reaction condition, reaction proceeded smoothly and provided 5-DTAF labeled QPG (QPG-5-DTAF), that was characterized by FT-IR, ^{1}H NMR, and fluorescent excitation and emission spectroscopy.

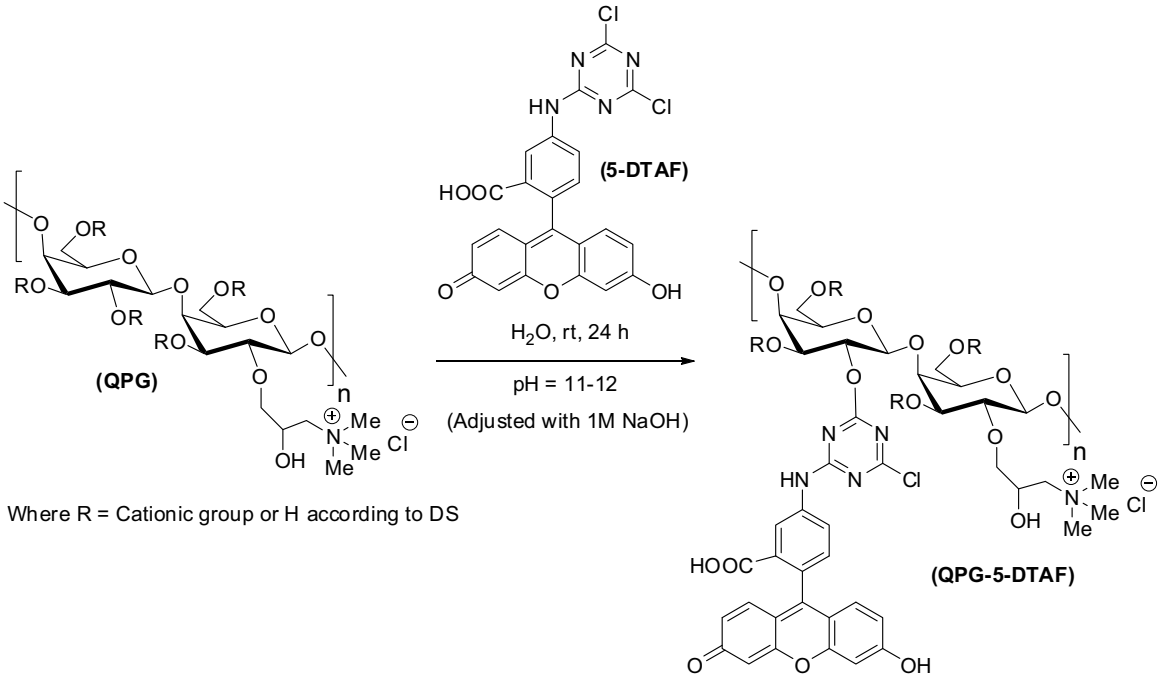

Scheme 2. Fluorescent labeling of QPG with 5-DTAF.

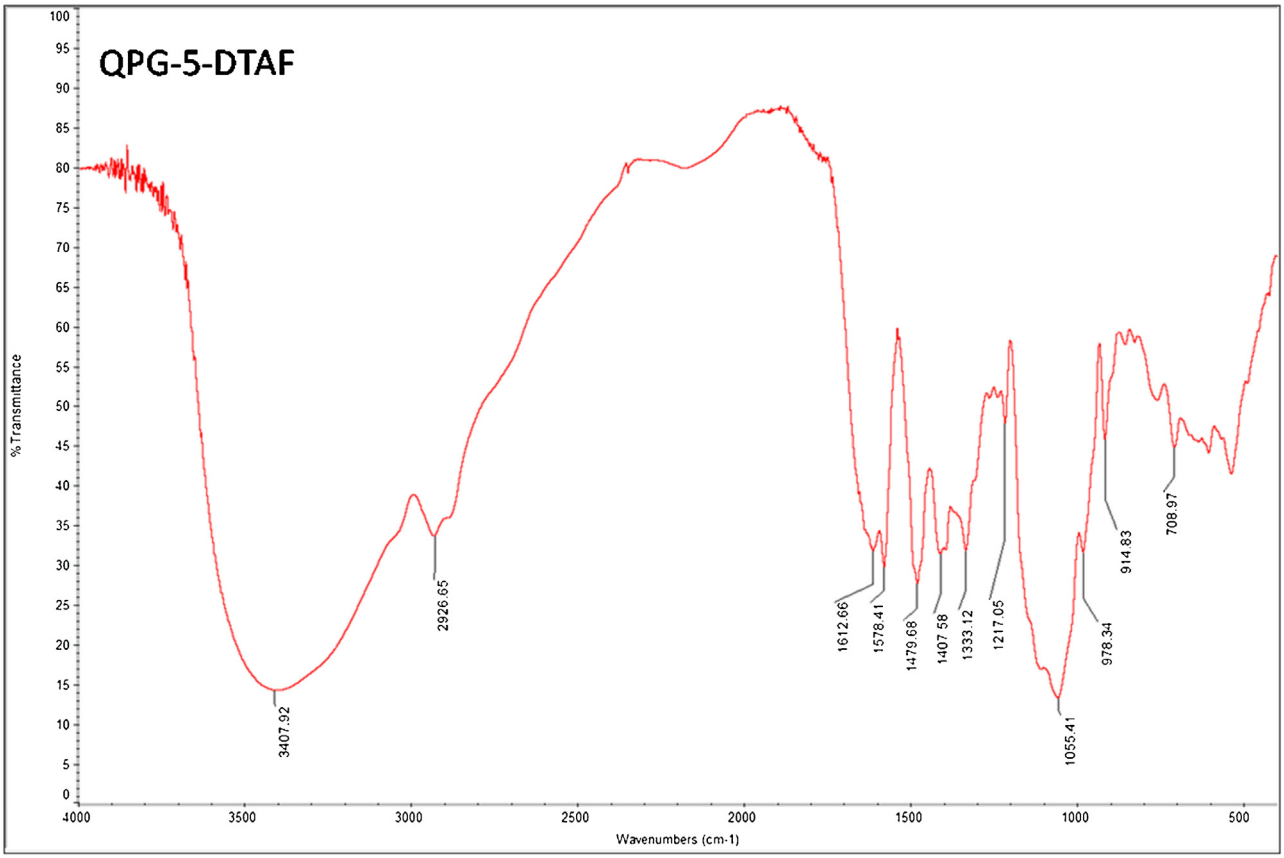

Fig. 4. FT-IR spectrum of QPG-5-DTAF.

3.4. Characterization of the QPG-5-DTAFby FT-IR, NMR, and fluorescent spectroscopy

The FT-IR spectrum of QPG-5-DTAF is shown in Fig. 4. From the FT-IR spectrum of QPG-5-DTAF, the new band at 1578 cm^{-1} is related to the N—H bending vibration of the secondary amine of attached 5-DTAF, the rest of the bands are similar when compared with the FT-IR of QPG, which is described in Fig. 2B. The appearance of the new band in the FT-IR spectrum of QPG-5-DTAF, confirms the insertion of 5-DTAF moiety onto the QPG.

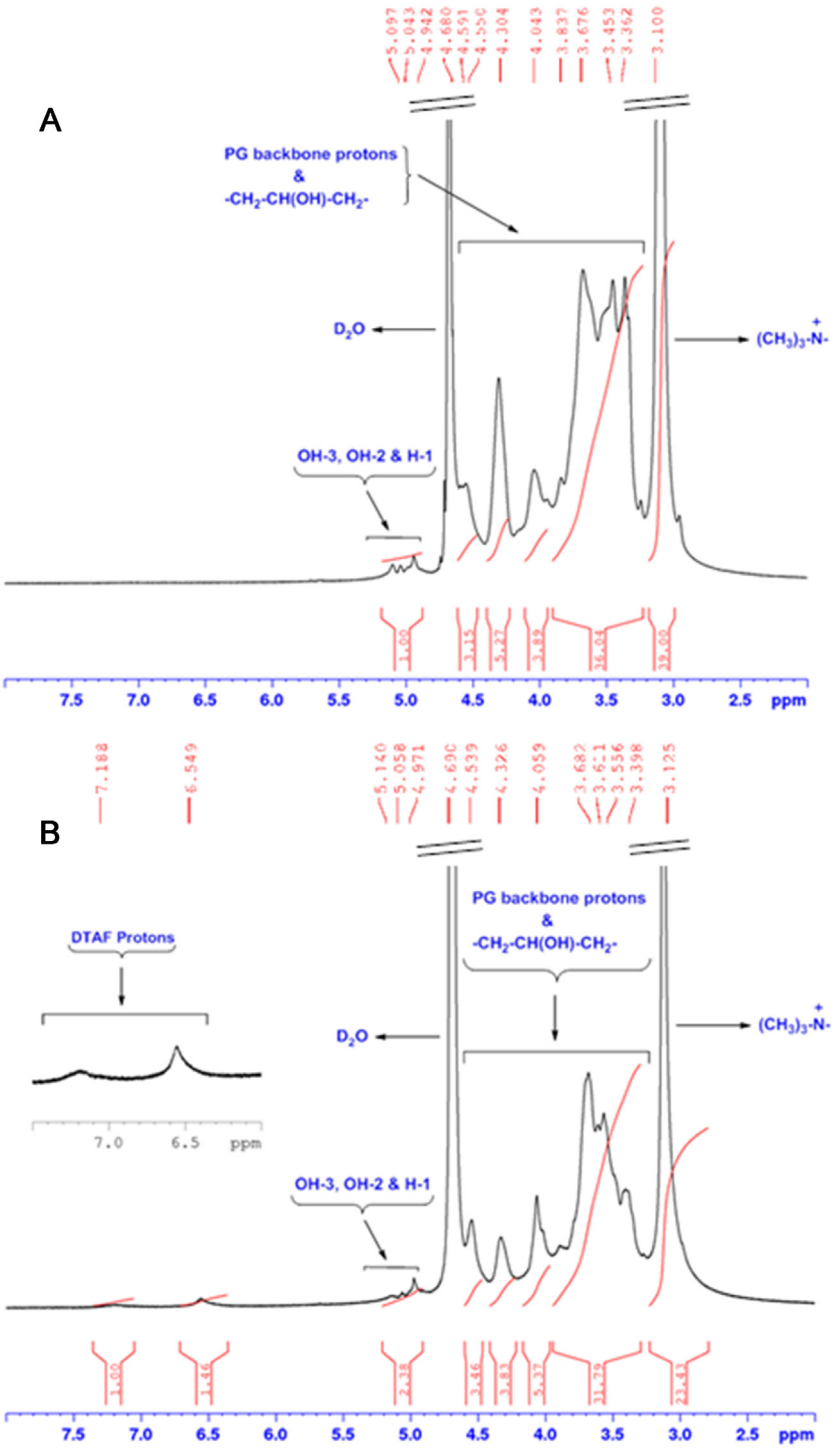

Fig. 5. ^{1}H NMR spectra of QPG (A) and QPG-5-DTAF (B).

A typical ^{1}H NMR spectra of QPG and QPG-5-DTAF in D_2O are presented in Fig. 5. In the QPG spectrum (Fig. 5A), the signals appearing between 5.07 and 4.96 ppm are assigned to OH-3, OH-2, and H-1. The PG protons (H-1 to H-5, H-6a,b, and OH-6) and quaternizing reagent protons (—CH_2—CH(OH)-CH_2-) appeared between 4.62 and 3.36 ppm. A relatively sharp and high intensity signal appeared at 3.13 ppm, which is attributed to 9 hydrogens of the quaternary ammonium group. In the case of QPG-5-DTAF (Fig. 5B), the new signals that appeared between 7.18 and 6.54 ppm are attributed to the DTAF protons at the attached QPG moiety; while these new signals are absent in the QPG spectrum, the rest of the signals of PG protons (H-1 to H-5, H-6a,b, and OH-6), quaternizing reagent protons (—CH_2—CH(OH)—CH_2—) and methyl protons of the quaternary ammonium ($^{+}N(CH_3)_3$) group appeared almost at the same chemical shifts, when compared with ^{1}H NMR of QPG. The appearance of the new peaks in the ^{1}H NMR spectrum of QPG-5-DTAF revealed the presence of the 5-DTAF moiety on the QPG. Particularly noteworthy is that the quaternary ammonium group of QPG was not affected during the fluorescent labeling with 5-DTAF.

The fluorescent excitation and emission spectra of QPG-5-DTAF are shown in Fig. 6. The excitation maxima (Fig. 6A) and emission

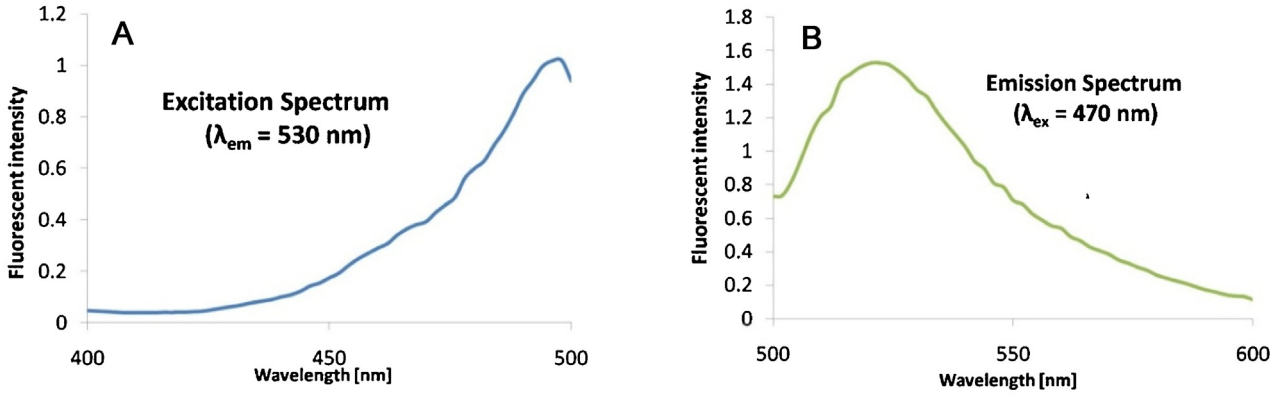

Fig. 6. Excitation (A) and Emission (B) spectra of QPG-5-DTAF.

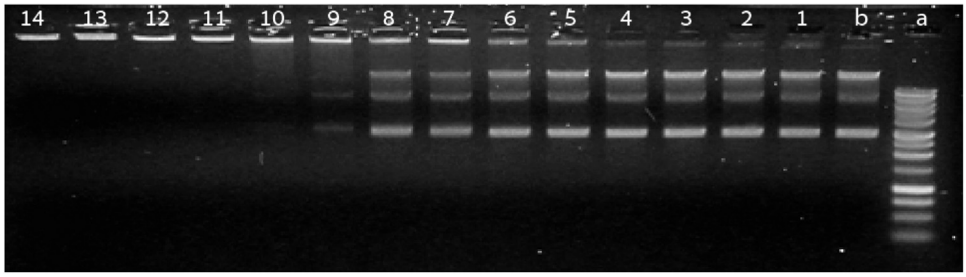

Fig. 7. Gel electrophoresis at different N/P ratios, lane a is 1Kb DNA ladder, and lane b is free DNA. Lanes 1–14: duplicates of the different ratios: (1-2) – 1/96, (3-4) – 1/48, (5-6) – 1/24, (7-8) – 1/12, (9-10) – 1/6, (11-12) – 1/4, (13-14) – 1/3.

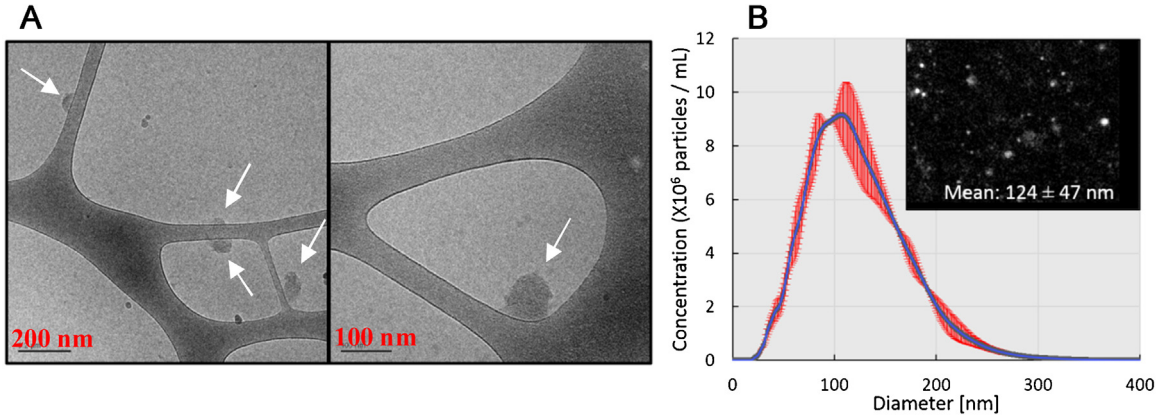

Fig. 8. Cryo-TEM images of QPG/pGFP complexes at N/P ratio of 1/3 (A). Particle concentration versus size distribution from NTA for QPG/pGFP complexes at N/P ratio of 1/3 (B). NTA video frame is presented inside the graph, as well as the mean diameter ± SDM.

maxima (Fig. 6B) measured in 0.1 M NaOH solution appeared at 498 nm and 522 nm, respectively. The appearance of excitation and emission bands in QPG-5-DTAF confirms the attachment of 5-DTAF to the QPG.

3.5. Self-assembly of QPG with pGFP

QPG is permanently positively charged and this feature enables the carrier to electrostatically interact with negatively charged molecules. The ability of QPG to interact electrostatically with DNA molecules in aqueous solution through self-assembly process, resulting in well-defined complexes, was evaluated using gel electrophoresis. QPG was dissolved in DDW, complexes at various N/P ratios were prepared. The complexes were subjected to gel electrophoresis and the migration profile was then analyzed (Fig. 7). Gel electrophoresis separates macromolecules on the basis of both charge and size. Therefore, immobilization of DNA can be attributed either to complex size or to the achievement of complete DNA charge neutralization. As can be seen in Fig. 7 lane b, free pGFP migrated in the gel according to its size and conformation. Moreover, with the increase in the N/P ratio, the pGFP migration capability was hindered and the amount of migrating free pGFP decreased. The N/P ratio where there is complete complexation of the pGFP with QPG can be seen in Fig. 7 lines 11–12, at N/P ratio of 1/4.

The morphology and size of complexes at a ratio of 1/3 were examined. Cryo-TEM technique was employed in order to visualize the system as an aqueous suspension; the desired hydrated state enables the examination of both size and morphology. cryo-TEM specimens with N/P ratio of 1/3 were prepared according to the protocol described in the method section. Representative cryo-TEM images are presented in Fig. 8A. Clear aggregation of low electron

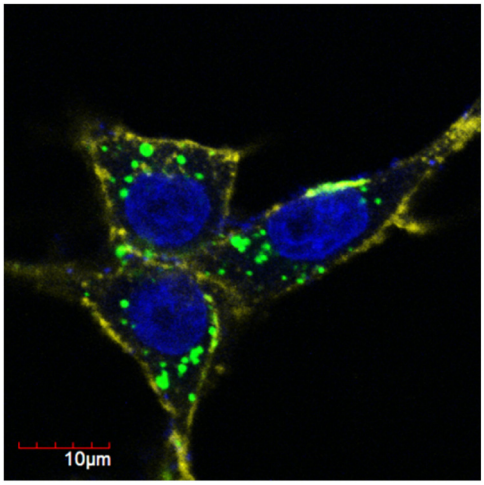

Fig. 9. Representative confocal image of C6 cellular path of QPG/pGFP complexes 24 h after exposure to the complexes. Bars represent 10 μm.

density materials was observed, which can be attributed to the complexes. Globular condensed complexes were observed in heterogeneous sizes, ranging from 60 to 160 nm. NTA technique was employed in order to examine the size of the complexes at N/P ratio of 1/3. NTA was found to well-characterize polydisperse nanosized particles (Filipe, Hawe, & Jiskoot, 2010). The NTA software is able to identify and track individual nanoparticles moving under Brownian motion; the velocity of the nanoparticle movement is used to calculate the hydrodynamic size according to the two-dimensional Stokes-Einstein equation (Dragovic et al., 2011). The NTA results are presented in Fig. 8B. A polydispersed population is observed as was found in the cryo-TEM images. The average hydrodynamic diameter was found to be 124 ± 47 nm. The average diameter that was found is within the range required for cellular endocytosis.

QPG/pGFP labeled complexes were introduced to C6 rat glioma cell line. A representative confocal image is presented in Fig. 9. Cells were recorded 24 h after exposure to the complexes. The labeled form of QPG (QPG-5-DTAF) was utilized in order to image the complexes (seen in green). The fluorescently labeled membrane can be seen in yellow and the nucleus in blue. The results indicate that after 24 h the complexes are inside the cell and are seen surrounding the nucleus.

4. Conclusions

We have prepared the QPGs with CHPTAC in the presence of aqueous NaOH solution under mild reaction conditions. The obtained QPG was successfully fluorescently labeled with 5-DTAF. The quaternary ammonium group is not affected during the florescent labeling. The results showed that the concentration of NaOH strongly influences the quaternization reaction; increasing or decreasing the NaOH concentration decreased the degree of substitution of QPG.Excess use of CHPTAC did not increase the degree of substitution of QPG. FT-IR, NMR, TGA and elemental analysis techniques were used to characterize the molecular structure of QPGs. Thermo gravimetric analysis (TGA) revealed that the thermal stability of QPGs was higher than that of PG. QPG was found to be able to interact electrostatically with pGFP in aqueous solution through a self-assembly process, resulting in globular condensed complexes with a nanometer scale size ranging from 60 to 160 nm. QPG/pGFP labeled complexes were introduced to C6 rat glioma cell line, the complexes were found to enter the cell and surround the nucleus within 24 h. The complexation of QPG with nucleic acids and their application to controlled release systems, targeted gene delivery, and drug delivery is currently under investigation in our laboratory, and will be published in forthcoming articles.

Competing interest

The authors declare no competing financial interest.

Acknowledgments

This work was supported by the Binational Science Foundation (BSF, United States–Israel, grant number 2009178) and Focal Technological Area (FTA) Program of the Israel National Nanotechnology Initiative (INNI). We wish to thank Dr. Nativ-Roth Einat (Ilse Katz Institute for Nanoscale Science and Technology) for the assistance in cryo-TEM imaging.

Appendix A. Supplementary data

Supplementary data associated with this article can be found, in the online version, at http://dx.doi.org/10.1016/j.carbpol.2016.05.015.

References

Abitbol, T., Palermo, A., Moran-Mirabal, J. M., & Cranston, E. D. (2013). Fluorescent labeling and characterization of cellulose nanocrystals with varying charge contents. *Biomacromolecules*, *14*, 3278–3284.

Cafaggi, S., Russo, E., Stefani, R., Leardi, R., Caviglioli, G., Parodi, B., et al. (2007). Preparation and evaluation of nanoparticles made of chitosan or *N*-trimethyl chitosan and a cisplatin-alginate complex. *Journal of Controlled Release*, *121*, 110–123.

Chaudhury, A., & Das, S. (2011). Recent advancement of chitosan-based nanoparticles for oral controlled delivery of insulin and other therapeutic agents. *APPS PharmSciTech*, *12*(March), 10–20.

Cho, J., Grant, J., Piquette-Miller, M., & Allen, C. (2006). Synthesis and physicochemical and dynamic mechanical properties of a water-soluble chitosan derivative as a biomaterial. *Biomacromolecules*, *7*, 2845–2855.

Cho, A., Choi, S.-H., Choi, H.-W., Kim, H.-S., Kim, W., Kim, D.-O., et al. (2013). Characterization of cationic dextrin prepared by ultra high pressure (UHP)-assisted cationization reaction. *Carbohydrate Polymers*, *97*, 130–137.

Dong, S., & Roman, M. (2007). Fluorescently labeled cellulose nanocrystals for bioimaging applications. *Journal of American Chemical Society*, *129*, 13810–13811.

Dragovic, R. A., Gardiner, C., Brooks, A. S., Tannetta, D. S., Ferguson, D. J. P., Hole, P., et al. (2011). Sizing and phenotyping of cellular vesicles using nanoparticle tracking analysis. *Nanomedicine: Nanotechnology, Biology and Medicine*, *7*, 780–788.

Ebringerova, A., Hromadkova, Z., Kacurakova, M., & Antal, M. (1994). Quaternizedxylans: synthesis and structural characterization. *Carbohydrate Polymers*, *24*, 301–308.

Edgar, K. J., Buchanan, C. M., Debenham, J. S., Rundquist, P. A., Seiler, B. D., Shelton, M. C., et al. (2001). Advances in cellulose ester performance and application. *Progress in Polymer Science*, *26*, 1605–1688.

Eliz, A. L., Aharon, A., Ramesh, C., Riki, G., Tamar, T., Jackson, P., et al. (2014). Quaternized starch-based carrier for siRNA delivery: from cellular uptake to gene silencing. *Journal of Controlled Release*, *185*, 109–120.

Fan, L., Cao Mi Gao, S., Wang, W., Peng, K., Tan, C., Wen, F., et al. (2012). Preparation and characterization of a quaternary ammonium derivative of pectin. *Carbohydrate Polymers*, *88*, 707–712.

Filipe, V., Hawe, A., & Jiskoot, W. (2010). Critical evaluation of nanoparticle tracking analysis (NTA) by NanoSight for the measurement of nanoparticles and protein aggregates. *Pharmaceutical Research*, *27*, 796–810.

Geresh, S., Dawadi, R. P., & Arad, S. (2000). Chemical modifications of biopolymers: quaternization of the extracellular polysaccharide of the red microalga Porphyridiumsp. *Carbohydrate Polymers*, *43*, 75–80.

Gil, E. S., Li, J., Xiao, H., & Lowe, T. L. (2009). Quaternary ammonium β-cyclodextrin nanoparticles for enhancing doxorubicin permeability across the In vitro blood-brain barrier. *Biomacromolecules*, *10*, 505–516.

Gong, Q., Wang, L.-Q., & Tu, K. (2006). In situ polymerization of starch with lactic acid in aqueous solution and the microstructure characterization. *Carbohydrate Polymers*, *64*, 501–509.

Gunning, A. P., Bongaerts, R. J. M., & Morris, V. J. (2009). Recognition of galactan components of pectin by galectin-3. *The FASEB Journal*, *23*, 415–424.

Hashem, M., Hauser, P., & Smith, B. (2003). Reaction efficiency for cellulose cationization using 3-chloro-2-hydroxypropyl trimethyl ammonium chloride. *Textile Research Journal*, *73*, 1017–1023.

Heinze, T., Haack, V., & Rensing, S. (2004). Starch derivatives of high degree of functionalization. 7. Preparation of cationic

2-hydroxypropyltrimethylammonium chloride starches. *Starch/Staerke*, *56*, 288–296.
Hoffman, A. S. (2002). Hydrogels for biomedical applications. *Advanced Drug Delivery Reviews*, *54*, 3–12.
Kavaliauskaite, R., Klimaviciute, R., & Zemaitaitis, A. (2008). Factors influencing production of cationic starches. *Carbohydrate Polymers*, *73*, 665–675.
Kim, H. W., Kim, B. R., & Rhee, Y. H. (2010). Imparting durable antimicrobial properties to cotton fabrics using alginate-quaternary ammonium complex nanoparticles. *Carbohydrate Polymers*, *79*, 1057–1062.
Niidei, T., Shiraki, H., Oshima, T., Baba, Y., Kamiya, N., & Gotoi, M. (2010). Quaternary ammonium bacterial cellulose for adsorption of proteins. *Solvent Extraction Research and Development: Japan*, *17*, 73–81.
Pal, S., Mal, D., & Singh, R. P. (2005). Cationic starch: an effective flocculating agent. *Carbohydrate Polymers*, *59*, 417–423.
Pal, S., Mal, D., & Singh, R. P. (2008). Characterization of cationic starch: an efficient flocculating agent. *Journal of Applied Polymer Science*, *108*, 2674–2681.
Prado, H., & Matulewicz, J. (2014). Cationization of polysaccharides: a path to greener derivatives with many industrial applications. *European Polymer Journal*, *52*, 53–75.
Sajomsang, W., Tantayanon, S., Tangpasuthadol, V., William, H., & Daly, W. H. (2009). Quaternization of *N*-aryl chitosan derivatives: synthesis, characterization, and antibacterial activity. *Carbohydrate Research*, *344*, 2502–2511.
Samal, S. K., Dash, M., Vlierberghe, S. V., Kaplan, D. L., Chiellini, E., Blitterswijk, C. V., et al. (2012). Cationic polymers and their therapeutic potential. *Chemical Society Reviews*, *41*, 7147–7194.
Solarek, D. B. (1986). In O. D. Wurzburg (Ed.), *Modified starches: properties and uses* (p. 113). Boca Raton, FL: CRC Press.
Song, Y., Sun, Y., & Zhang, X. (2008). Homogeneous quaternization of cellulose in NaOH/urea aqueous solutions as gene carriers. *Biomacromolecules*, *9*, 2259–2264.
Sonia, T. A., & Sharma, C. P. (2011). Chitosan and its derivatives for drug delivery perspective. *Advanced Polymer Science*, *243*, 23–54.
Synytsya, A., Čopiková, J., Marounek, M., Mlčochová, P., Sihelniková, L., Skoblya, S., et al. (2004). *N*-Octadecylpectinamide, a hydrophobic sorbent based on modification of highly methoxylated citrus pectin. *Carbohydrate Polymers*, *56*, 169–179.
Wang, Y., & Xie, W. (2010). Synthesis of cationic starch with a high degree of substitution in an ionic liquid. *Carbohydrate Polymers*, *80*, 1172–1177.
Wang, P.-X., Wub, X.-L., Dong-hua, X., Kun, X., Ying, T., Xi-bing, D., et al. (2009). Preparation and characterization of cationic corn starch with a high degree of substitution in dioxane-THF-water media. *Carbohydrate Research*, *344*, 851–855.
Yu, H., Huang, Y., Ying, H., & Xiao, C. (2007). Preparation and characterization of a quaternary ammonium derivative of konjacglucomannan. *Carbohydrate Polymers*, *69*, 29–40.
Yudovin-Farber, I., & Domb, A. J. (2007). Cationic polysaccharides for gene delivery. *Materials Science and Engineering C*, *27*, 595–598.